

Proposal for a Quantum Test of the Weak Equivalence Principle with Entangled Atomic Species

Remi Geiger*

*LNE-SYRTE, Observatoire de Paris, Sorbonne Université,
PSL Université Paris, CNRS, 61 avenue de l'Observatoire, 75014 Paris, France*

Michael Trupke[†]

*Vienna Center for Quantum science and technology (VCQ), Faculty of Physics, Research Platform TURIS,
University of Vienna, A-1090 Vienna, Austria*



(Received 16 June 2017; published 25 January 2018)

We propose an experiment to test the weak equivalence principle (WEP) with a test mass consisting of two entangled atoms of different species. In the proposed experiment, a coherent measurement of the differential gravity acceleration between the two atomic species is considered, by entangling two atom interferometers operating on the two species. The entanglement between the two atoms is heralded at the initial beam splitter of the interferometers through the detection of a single photon emitted by either of the atoms, together with the impossibility of distinguishing which atom emitted the photon. In contrast to current and proposed tests of the WEP, our proposal explores the validity of the WEP in a regime where the two particles involved in the differential gravity acceleration measurement are not classically independent, but entangled. We propose an experimental implementation using ^{85}Rb and ^{87}Rb atoms entangled by a vacuum stimulated rapid adiabatic passage protocol implemented in a high-finesse optical cavity. We show that an accuracy below 10^{-7} on the Eötvös parameter can be achieved.

DOI: [10.1103/PhysRevLett.120.043602](https://doi.org/10.1103/PhysRevLett.120.043602)

The current understanding of gravity is formulated by the theory of general relativity which has been proven to accurately describe many astronomical phenomena. The weak equivalence principle (WEP), also known as the universality of free fall, represents one of the three pillars of the Einstein equivalence principle, which was the basis of the elaboration of general relativity [1]. According to Damour [2], the equivalence “principle” is not satisfactory, as it sets an absolute structure for fundamental coupling constants (e.g., the fine-structure constant), in contrast to how physics (and relativity in particular) is constructed, i.e., avoiding the assumption of absolute structures. Unification theories, which aim at describing gravity and the three interactions of the standard model within a single mathematical framework, therefore commonly imply violations of the equivalence principle. WEP tests thus represent key probes in the search of new physical phenomena [2]. As the types of WEP violations, as well as the levels at which they could occur, are theoretically elusive, an experiment with improved accuracy or involving a different type of test mass might therefore point towards new physics [2].

WEP tests are quantified by the Eötvös parameter $\eta = 2(a_A - a_B)/(a_A + a_B)$, which deviates from zero if the accelerations a_A and a_B of the two bodies are different in a given gravitational field. WEP has been tested at the level of 10^{-13} uncertainty on the Eötvös parameter in continuously improved experiments involving torsion balances [3] or lunar

laser ranging [4]. The first results of the MICROSCOPE experiment [5], which involves two free-falling macroscopic differential accelerometers, show the validity of WEP at the level of 2×10^{-14} . Apart from these high-precision experiments involving macroscopic masses, efforts are also being pursued to test the WEP with microscopic or exotic particles. These efforts started with experiments involving electrons [6] and neutron interferometers [7–9]. More recently, several results with cold atoms have been reported [10–16], together with proposals for improved tests [17–19]. Experiments using antimatter are also being developed [20,21].

The WEP and the role of inertial and gravitational masses in quantum mechanics have been studied theoretically in numerous works; see, e.g., Refs. [22,23]. It was shown recently in Ref. [24] that the validity of the equivalence principle for classical objects does not imply the validity of its quantum formulation, i.e., the equivalence between inertial and gravitational mass operators. Such considerations point towards new experimental approaches involving quantum test particles described by superposition states of internal degrees of freedom, e.g., as proposed in Ref. [25]. Very recently, an atom interferometry test of such a quantum formulation of the equivalence principle has been performed by measuring the free-fall acceleration of an atom in a superposition of different internal energy states [16].

In this Letter we propose a test of the WEP with a fundamentally different type of object than in previous or

ongoing experiments, namely two entangled atoms of different species. The experiment considers the comparison of the free-fall acceleration of an atom \mathcal{A} when it is entangled with a different atomic species \mathcal{B} to the free-fall acceleration of the atoms without entanglement. We describe a particular implementation with ^{85}Rb and ^{87}Rb atoms and an entangling process based on a vacuum stimulated rapid adiabatic passage protocol implemented in a high-finesse optical cavity.

The concept of our proposal relies on a vertical atom interferometer in which atomic species \mathcal{A} and \mathcal{B} are entangled. The entanglement is heralded at the first beam splitter of the interferometer by the detection of a single photon. The scheme is related to the seminal work in Refs. [26,27], but operates here on freely propagating, distinguishable atoms instead of trapped, identical particles. In the event of the emission of a single photon from one of the two atoms in the direction of a photon detector, and assuming that it is not possible to distinguish which atom emitted the photon, a detection event will herald a superposition state: Atom \mathcal{A} acquires the momentum $\hbar\vec{k}$ (\mathcal{A} emitted the photon of wave vector \vec{k}) and atom \mathcal{B} is left unperturbed, or vice versa. The corresponding entangled state can be written as

$$|\psi\rangle = \frac{1}{\sqrt{2}}(|\mathcal{A}, \hbar\vec{k}; \mathcal{B}, \vec{0}\rangle + e^{i\phi}|\mathcal{A}, \vec{0}; \mathcal{B}, \hbar\vec{k}\rangle). \quad (1)$$

The beam splitter thus creates a superposition of the momenta of the two atomic species \mathcal{A} and \mathcal{B} , with ϕ a fixed (nonrandom) phase in the case of a coherent superposition. To complete the interferometer, the two paths produced at the first beam splitter are subsequently manipulated with conventional atom optics (e.g., two-photon Raman transitions [28]) in order for the paths of each species to interfere. Single atom detectors are finally used to probe the atomic interference at the interferometer output.

We focus in this Letter on a particular implementation of this idea using ^{85}Rb and ^{87}Rb atoms, as sketched in Fig. 1. To entangle the two atoms, we propose to employ a vacuum stimulated Raman adiabatic passage (vSTIRAP) protocol [29], where the detection of a single photon exiting a high-finesse optical ring cavity heralds the entangled state of Eq. (1). The cavity is on resonance with a mode of frequency ω_c . The two atoms are initialized in one of their two hyperfine ground states, respectively, $|F=3\rangle$ for $\mathcal{A} = ^{85}\text{Rb}$ and $|F=2\rangle$ for $\mathcal{B} = ^{87}\text{Rb}$; see Fig. 1(b). The vSTIRAP process is triggered at time $t = t_0$ by a pulse of two pump laser beams at frequencies $\omega_p^{\mathcal{A}}$ and $\omega_p^{\mathcal{B}}$ (red and blue vertical arrows), which fulfill the two-photon Raman resonance condition for each atom: $\omega_p^\alpha - \omega_c = G^\alpha + \omega_R^\alpha$, where G^α is the hyperfine splitting frequency, and ω_R^α is the two-photon recoil frequency, with $\alpha = \mathcal{A}, \mathcal{B} = ^{85}\text{Rb}, ^{87}\text{Rb}$ [30]. Assuming that the probability of the adiabatic passage for each atom is small [26,27], the vSTIRAP process will in all likelihood deposit at most a single photon into the cavity. The photon can then escape the cavity while one of

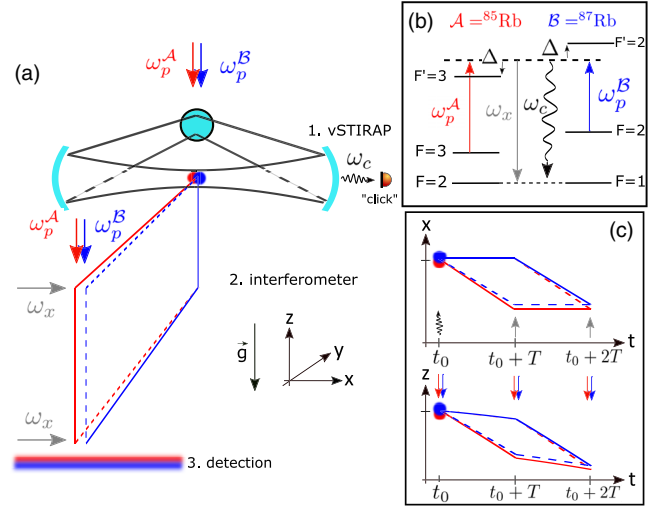


FIG. 1. Implementation with ^{85}Rb and ^{87}Rb atoms and a vSTIRAP protocol to realize the entangling beam splitter. (a) General sketch of the experiment: the atoms are laser cooled and then released in a high-finesse optical cavity made of three mirrors lying in the (xy) plane. During the vSTIRAP process, a photon is extracted from the pump beam (red and blue arrows for ^{85}Rb and ^{87}Rb , respectively), and a photon is emitted into the cavity mode. The emitted photon (frequency ω_c) is detected at one output of the cavity (“click”). (b) Energy levels of the atoms subject to two-photon Raman transitions. The high-finesse cavity is resonant for a mode of frequency ω_c . The vSTIRAP process is initiated at time $t = t_0$ by a pulse of the pump beams of frequency $\omega_p^{\mathcal{A},\mathcal{B}}$. The gray arrow represents a laser beam (frequency $\omega_x = \omega_c$) used to perform the Raman transitions in the mirror pulse and final beam splitter pulse. (c) Space-time diagrams of the atom interferometer in the x and z directions. In (a) and (c), the difference in recoil velocities between ^{85}Rb and ^{87}Rb has been exaggerated to 10% (instead of 2.3%). In the bottom of (c), gravity has been reduced to $g = 0.01 \text{ m s}^{-2}$ in order to highlight the recoil effect.

the atoms is transferred from one hyperfine state to the other [29,31]. If the photon emission of both atomic species can be made to have the same envelope and frequency, then a detection event will herald the desired entangled state.

In view of the WEP test, we aim to measure the gravitational acceleration with the atom interferometer, requiring a vertical accelerometer [28]. Therefore, at least one of the light beams realizing the Raman transition must have a projection on the gravity direction (z). We choose a configuration where the cavity is horizontal (xy plane in Fig. 1) and where the pump beams are aligned with gravity. As a consequence, the beam splitter operates in two dimensions, with a transfer of momentum $\hbar\vec{k}_{\text{tot}} \equiv \hbar(k_x\hat{x} - k_z\hat{z})$ along the \hat{x} and \hat{z} direction, with $k_x = \omega_c/c$ (k_z) the wave vector of the cavity (pump) photon. The remaining part of the interferometer is a typical Mach-Zehnder configuration [28], apart from the fact that the mirror and final beam splitter pulses are two-dimensional in the momentum transfer; see Fig. 1(c).

After the last beam splitter pulse occurring at time $t = t_0 + 2T$, the detection of each single-atom state can be performed by fluorescence detection with a photodiode [32], or by imaging using a light sheet detector [33].

We compute the atom interferometer phase shift following the path integral approach [34]. In atom interferometers using two-photon Raman transitions, the phase of the interferometer originates from the relative phase between the Raman lasers $\phi(t)$, which is imprinted on the diffracted atomic wave by the different Raman pulses [35,36]. More precisely, the phase shift imprinted on atom $\alpha = \mathcal{A}, \mathcal{B}$ by a light pulse is $\phi_\alpha(t) = \vec{k}_{\text{tot}}^\alpha \cdot \vec{r}^\alpha(t) + \varphi_0^\alpha(t)$, with $\vec{r}^\alpha(t)$ the position of the atom in the laboratory frame holding the lasers and the cavity, and $\varphi_0^\alpha(t)$ a phase offset associated with the change of the internal energy state. Assuming that all Raman lasers are phase locked [i.e., red (gray) and blue (gray) lasers in Fig. 1], we can leave aside the φ_0 term and neglect the finite duration of the Raman pulse ($\sim 10 \mu\text{s}$ typically). The laser phase can then be written more explicitly as $\phi^\alpha(t) = -k_x x_\alpha(t) - k_z z_\alpha(t)$. Note that k_x is the same for both atoms (gray arrow); the relative difference in k_z is $\sim 10^{-5}$ (difference in hyperfine splitting between ^{85}Rb and ^{87}Rb) and will be omitted from now on [37].

After the vSTIRAP process, the two-particle state reads

$$|\psi(t_0)\rangle = \frac{1}{\sqrt{2}}(|\mathcal{A}, \hbar\vec{k}_{\text{tot}}; \mathcal{B}, \vec{0}\rangle e^{i\phi_0^{\mathcal{A}}} + |\mathcal{A}, \vec{0}; \mathcal{B}, \hbar\vec{k}_{\text{tot}}\rangle e^{i\phi_0^{\mathcal{B}}}), \quad (2)$$

with $\phi_0^\alpha \equiv \phi^\alpha(t_0)$. Note that we have treated the phase shift imprinted on the atom during the vSTIRAP process as for a conventional Raman transition, although the emission of the photon occurs in the vacuum of the cavity mode [38]. In the Raman process, the change of momentum $\vec{0} \leftrightarrow \vec{k}_{\text{tot}}$ is accompanied by a change of the hyperfine state of the atom [39], which we omit in Eq. (2) to simplify the notations.

After the mirror pulse at time $t_0 + T$, the state reads

$$|\psi(t_0 + T)\rangle = \frac{1}{\sqrt{2}}[|\mathcal{A}, \vec{0}; \mathcal{B}, \hbar\vec{k}_{\text{tot}}\rangle e^{i\phi_0^{\mathcal{A}}} e^{i(\phi_T^{\mathcal{B}} - \phi_T^{\mathcal{A}})} + |\mathcal{A}, \hbar\vec{k}_{\text{tot}}; \mathcal{B}, \vec{0}\rangle e^{i\phi_0^{\mathcal{B}}} e^{i(\phi_T^{\mathcal{A}} - \phi_T^{\mathcal{B}})}], \quad (3)$$

with $\phi_T^\alpha \equiv \phi^\alpha(t_0 + T)$ the relative Raman laser phase at time $t_0 + T$. The last beam splitter occurring at $t_0 + 2T$ acts globally on both atoms [27], which results in the output state

$$|\psi(t_0 + 2T)\rangle = \frac{1}{2\sqrt{2}}[|\mathcal{A}, \vec{0}; \mathcal{B}, \vec{0}\rangle (ie^{i(\varphi - \phi_{2T}^{\mathcal{A}})} + ie^{i(\Psi - \phi_{2T}^{\mathcal{B}})}) + |\mathcal{A}, \hbar\vec{k}_{\text{tot}}; \mathcal{B}, \hbar\vec{k}_{\text{tot}}\rangle (ie^{i(\varphi + \phi_{2T}^{\mathcal{B}})} + ie^{i(\Psi + \phi_{2T}^{\mathcal{A}})}) + |\mathcal{A}, \vec{0}; \mathcal{B}, \hbar\vec{k}_{\text{tot}}\rangle (i^2 e^{i(\varphi - \phi_{2T}^{\mathcal{A}} + \phi_{2T}^{\mathcal{B}})} + e^{i\Psi}) + |\mathcal{A}, \hbar\vec{k}_{\text{tot}}; \mathcal{B}, \vec{0}\rangle (e^{i\varphi} + i^2 e^{i(\Psi + \phi_{2T}^{\mathcal{A}} - \phi_{2T}^{\mathcal{B}})})], \quad (4)$$

where $\varphi = \phi_0^{\mathcal{B}} + \phi_T^{\mathcal{A}} - \phi_T^{\mathcal{B}}$ and $\Psi = \phi_0^{\mathcal{A}} + \phi_T^{\mathcal{B}} - \phi_T^{\mathcal{A}}$.

The detection of the four possible states at the interferometer output can be performed by fluorescence detection (light sheets in Fig. 1), which resolves the two hyperfine states of each atom [39]. For example, the probability of detecting atom \mathcal{A} and atom \mathcal{B} in the output port corresponding to the null momentum (projector on state $|\mathcal{A}, \vec{0}; \mathcal{B}, \vec{0}\rangle$) is given by

$$P_{00} = |\langle \mathcal{A}, \vec{0}; \mathcal{B}, \vec{0} | \psi(t_0 + 2T) \rangle|^2 = \frac{1}{8} |1 + e^{i(\Phi_{\mathcal{A}} - \Phi_{\mathcal{B}})}|^2, \quad (5)$$

with $\Phi_\alpha = \phi_0^\alpha - 2\phi_T^\alpha + \phi_{2T}^\alpha$.

The expression of the phase shift Φ_α is the same as in a traditional three light pulse interferometer [34]. However, in contrast to two classically independent interferometers that would operate in parallel on atom \mathcal{A} and atom \mathcal{B} , the phase of the entangled interferometer, $\Delta\Phi \equiv \Phi_{\mathcal{A}} - \Phi_{\mathcal{B}}$, is determined by the phase shifts experienced by both atoms, as a result of two-particle interferometry [40,41]. The entanglement between the two interferometers can thus be verified experimentally by applying controlled phase shifts on the relative phase of the (phase-locked) Raman lasers: while a phase shift applied to only one pair of lasers (say, for \mathcal{A}) affects the mutual signal P_{00} , the same phase shift applied on both pairs of lasers should not affect P_{00} .

Finally, $\Delta\Phi$ results from the terms in Eq. (4), and writing the trajectories of the atoms as $x^\alpha(t) = x_0^\alpha + v_{x0}^\alpha(t - t_0) + a_x^\alpha(t - t_0)^2/2$ and $z^\alpha(t) = z_0^\alpha + v_{z0}^\alpha(t - t_0) - g_z^\alpha(t - t_0)^2/2$, we obtain

$$\Delta\Phi = k_z(g_z^{\mathcal{A}} - g_z^{\mathcal{B}})T^2 + k_x(a_x^{\mathcal{A}} - a_x^{\mathcal{B}})T^2, \quad (6)$$

which reflects the bidirectional acceleration sensitivity of the interferometer. Provided that the experiment is not constantly accelerated in the horizontal direction with respect to the freely falling atoms ($a_x^\alpha = 0$), the second term vanishes on average. The main phase shift of the interferometer, $\Delta\Phi_{\text{WEP}} \equiv k_z(g_z^{\mathcal{A}} - g_z^{\mathcal{B}})T^2$, represents a coherent measurement of the difference in the gravitational acceleration between the two atoms.

Details of implementation and expected sensitivity.— The design of the experiment is driven by the need for indistinguishability of the emitted photon during the vSTIRAP process, and of the two atoms in the interferometer up to the last beam splitter. On the technical aspects, the design must take into account (i) the preparation of two cold atoms of ^{85}Rb and ^{87}Rb with high probability, (ii) the design of the high-finesse ring cavity, (iii) the optical access for the laser beams realizing the mirror and final beam splitter pulses, and (iv) the detection of the two atoms. We consider atoms loaded in the cavity mode and exiting the cavity for the second and third interferometer pulses. This requires a sufficient interrogation time, set to $T = 50$ ms in the following.

The first step consists of preparing two cold (\sim few μK) ^{85}Rb and ^{87}Rb atoms, which can be achieved in microscopic

dipole traps operating in the collisional blockade regime [32,42,43]. The ^{85}Rb and ^{87}Rb atoms are prepared in the states $|F = 3, m_F = 3\rangle$ and $|F = 2, m_F = 2\rangle$, respectively, and driven with individual, π -polarized pump beams. We envisage a ring cavity with coupling strength, field amplitude decay, and atomic decay rates $\{g, \kappa, \gamma\}/2\pi = \{2.24, 0.5, 2.9\}$ MHz for the $|F = 2, m_F = 2\rangle \leftrightarrow |F' = 3, m'_F = 3\rangle$ transition of the D_1 line of ^{85}Rb [31]. The cavity is also coupled to the $|F = 1, m_F = 1\rangle \leftrightarrow |F' = 2, m'_F = 2\rangle$ transition of the D_1 line of ^{87}Rb . The coupling strength g is reduced to $2\pi \times 2.12$ MHz for ^{87}Rb because of its slightly smaller transition matrix element. The cavity is detuned by $\Delta/2\pi = 1.367$ GHz from the ^{85}Rb transition and by $-\Delta$ from the ^{87}Rb line, leading to identical emission frequencies. This setting is chosen as neighboring transitions are either far detuned or forbidden.

Using a three-level master equation approach, we calculate the dynamics of the vSTIRAP process, and confirm that the power envelopes of the photons emitted by the two atomic species can be made almost perfectly indistinguishable by tuning the Rabi frequencies of the two processes [37,44,45]. We further find that the efficiency of the processes and the probability of spontaneous emission can be tuned to achieve a workable success probability $P_S = 2 \times P_{\text{stim}} \times (1 - P_{\text{stim}}) \times P_{\text{coll}} \times (1 - P_{\text{spont}})^2$, where P_{stim} , P_{coll} , and P_{spont} indicate the probabilities for stimulated emission, photon collection, and spontaneous emission, respectively. We also extract the probability for false-positive detection (both atoms emit a photon, but only one is detected), $P_F = P_{\text{stim}}^2 \times P_{\text{coll}} \times (1 - P_{\text{coll}})$, where we assume number-resolving photon detectors [31,46]. From the numerical calculations we find the best ratio $P_{\text{stim}}/P_{\text{spont}} \approx 3.2$ for $P_{\text{stim}} < 0.2$. In this regime there is therefore a simple trade-off between success probability and false-positive detection. For example, if we assume $P_{\text{coll}} = 0.4$ and $P_{\text{stim}} = 0.1$ (Ref. [47]), then $P_S = 7.0\%$ and $P_F = 0.26\%$ [37]. Spontaneous emission is not problematic as such, since it will in all likelihood lead to a loss of the affected atom from the spatial or temporal detection windows.

Ensuring that the two atoms couple in the same way to the cavity mode requires their separation to be less than the mode waist ($\sim 40 \mu\text{m}$) in the radial direction and less than the cavity mode Rayleigh length in the longitudinal direction (\sim few mm). This is not a concern for atoms at few μK temperatures and a free evolution time $t_0 \sim 1$ ms between the atom preparation and the vSTIRAP pulse.

Because of the different masses of the two atoms, the recoil is different by 2.3% for the two species, which results in different paths followed by the particles (this effect is exaggerated in Fig. 1). For $T = 50$ ms, the maximum displacement between the two species within one interferometer path is $\approx 5 \mu\text{m}$ [48].

We conclude by estimating the sensitivity that could be achieved in a WEP test. The interferometer fringes can be

reconstructed shot after shot by varying the Raman laser relative phase for one species (e.g., before the last beam splitter), allowing one to extract $\Delta\Phi_{\text{WEP}}$. Assuming a single-atom quantum projection noise limited sensitivity [32], the acceleration sensitivity is given by $\sigma_{\text{WEP}} \approx 1/(k_z T^2 \sqrt{N})$, where N is the number of measurements. With $N = 10^4$ successful measurements (10 mrad phase sensitivity) and $T = 50$ ms, a differential acceleration sensitivity $\sim 5 \times 10^{-7} \text{ m s}^{-2}$ can be reached, corresponding to a potential sensitivity $\sim 5 \times 10^{-8}$ on the Eötvös parameter. Note that vibration noise is expected to have a negligible effect as it is common to both interferometers [see Eq. (6)]. Further measurements can then be performed independently with one species at a time to extract the values of the gravitational acceleration separately for each species, and to investigate systematic effects [49].

The effect of entanglement on the free fall can thus be directly assessed by comparing the differential gravity obtained with the entangled atoms ($g^A - g^B$ in $\Delta\Phi_{\text{WEP}}$) to that obtained with the classically independent atoms (g^A and g^B measured independently).

WEP tests have so far relied on a differential measurement between two classically independent proof masses. This includes experiments with cold atom interferometers [11–16], which explore the validity of the WEP in a different regime than experiments involving macroscopic objects, because the measurement principle involves matter-wave interference, and therefore rely on superpositions of quantum degrees of freedom. For example, the recent result reported in Ref. [16] uses an atom in an incoherent superposition of two internal energy states separated by $\sim 30 \mu\text{eV}$, allowing one to probe new possible WEP violations [24]. Our proposal makes a conceptual stride beyond previous works, by enforcing entanglement between two atomic species of different mass (~ 2 GeV energy difference), allowing one to probe directly the effect of entanglement on the free fall. More specifically, our scheme could, for example, be used to assess the quantum formulation of the WEP presented in Ref. [24] at the scale of 2 GeV [50].

To the best of our knowledge, there is currently no theoretical model which addresses the question of whether or not the presence of entanglement in a system could lead to a violation of the WEP at a given level of accuracy. In general, WEP tests involving new types of physical objects, such as matter waves or antimatter, are motivated by the qualitatively different nature of the involved proof masses, rather than by a consensual theoretical argument predicting a violation in such systems. Our proposal follows this approach by aiming for a test of a foundational principle of physics with a qualitatively new system not considered before [51].

Beyond a conceptually new type of WEP test, our proposal can be used for a test of Bell's inequalities with free-falling massive particles of different species.

Following Ref. [52], a correlation coefficient E can be formed from the measurement of the four joint probabilities associated to the four modes appearing in Eq. (4). It reads $E = V \cos(\Delta\Phi) \simeq V \cos[k_z T^2 (g_z^A - g_z^B)]$ and can be interpreted as a measure for a Bell test in the presence of gravity.

We thank P. Wolf, C. Garrido Alzar, Y. Sortais, A. Landragin, A. Browaeys, F. Pereira Dos Santos, J.-P. Uzan, and Č. Brukner for fruitful discussions.

*remi.geiger@obspm.fr

†michael.trupke@univie.ac.at

- [1] C. M. Will, *Living Rev. Relativity* **9**, 3 (2006).
- [2] T. Damour, *Classical Quantum Gravity* **29**, 184001 (2012).
- [3] T. A. Wagner, S. Schlamminger, J. H. Gundlach, and E. G. Adelberger, *Classical Quantum Gravity* **29**, 184002 (2012).
- [4] J. G. Williams, S. G. Turyshev, and D. H. Boggs, *Phys. Rev. Lett.* **93**, 261101 (2004).
- [5] P. Touboul *et al.*, *Phys. Rev. Lett.* **119**, 231101 (2017).
- [6] F. C. Witteborn and W. M. Fairbank, *Phys. Rev. Lett.* **19**, 1049 (1967).
- [7] R. Colella, A. W. Overhauser, and S. A. Werner, *Phys. Rev. Lett.* **34**, 1472 (1975).
- [8] U. Bonse and T. Wroblewski, *Phys. Rev. Lett.* **51**, 1401 (1983).
- [9] H. Abele and H. Leeb, *New J. Phys.* **14**, 055010 (2012).
- [10] S. Fray, C. A. Diez, T. W. Hänsch, and M. Weitz, *Phys. Rev. Lett.* **93**, 240404 (2004).
- [11] M. G. Tarallo, T. Mazzoni, N. Poli, D. V. Sutyryn, X. Zhang, and G. M. Tino, *Phys. Rev. Lett.* **113**, 023005 (2014).
- [12] D. Schlippert, J. Hartwig, H. Albers, L. L. Richardson, C. Schubert, A. Roura, W. P. Schleich, W. Ertmer, and E. M. Rasel, *Phys. Rev. Lett.* **112**, 203002 (2014).
- [13] L. Zhou, S. Long, B. Tang, X. Chen, F. Gao, W. Peng, W. Duan, J. Zhong, Z. Xiong, J. Wang, Y. Zhang, and M. Zhan, *Phys. Rev. Lett.* **115**, 013004 (2015).
- [14] A. Bonnin, N. Zahzam, Y. Bidel, and A. Bresson, *Phys. Rev. A* **92**, 023626 (2015).
- [15] X.-C. Duan, X.-B. Deng, M.-K. Zhou, K. Zhang, W.-J. Xu, F. Xiong, Y.-Y. Xu, C.-G. Shao, J. Luo, and Z.-K. Hu, *Phys. Rev. Lett.* **117**, 023001 (2016).
- [16] G. Rosi, G. D’Amico, L. Ciacciapuoti, F. Sorrentino, M. Prevedelli, M. Zych, C. Brukner, and G. M. Tino, *Nat. Commun.* **8**, 15529 (2017).
- [17] S. Dimopoulos, P. W. Graham, J. M. Hogan, and M. A. Kasevich, *Phys. Rev. Lett.* **98**, 111102 (2007).
- [18] G. Varoquaux, R. A. Nyman, R. Geiger, P. Cheinet, A. Landragin, and P. Bouyer, *New J. Phys.* **11**, 113010 (2009).
- [19] B. Altschul *et al.*, *Adv. Space Res.* **55**, 501 (2015).
- [20] P. Debu, *Hyperfine Interact.* **212**, 51 (2012).
- [21] A. Kellerbauer *et al.*, *Nucl. Instrum. Methods Phys. Res., Sect. B* **266**, 351 (2008).
- [22] L. Viola and R. Onofrio, *Phys. Rev. D* **55**, 455 (1997).
- [23] E. Kajari, N. L. Harshman, E. M. Rasel, S. Stenholm, G. Süßmann, and W. P. Schleich, *Appl. Phys. B* **100**, 43 (2010).
- [24] M. Zych and C. Brukner, [arXiv:1502.00971](https://arxiv.org/abs/1502.00971).
- [25] P. J. Orlando, R. B. Mann, K. Modi, and F. A. Pollock, *Classical Quantum Gravity* **33**, 19LT01 (2016).
- [26] C. Cabillo, J. I. Cirac, P. García-Fernández, and P. Zoller, *Phys. Rev. A* **59**, 1025 (1999).
- [27] L. Slodicka, G. Hétet, N. Röck, P. Schindler, M. Hennrich, and R. Blatt, *Phys. Rev. Lett.* **110**, 083603 (2013).
- [28] M. Kasevich and S. Chu, *Phys. Rev. Lett.* **67**, 181 (1991).
- [29] M. Hennrich, T. Legero, A. Kuhn, and G. Rempe, *Phys. Rev. Lett.* **85**, 4872 (2000).
- [30] We neglect here the Doppler effect originating from the velocity of the atom in the direction of the beams.
- [31] T. Wilk, S. C. Webster, H. P. Specht, G. Rempe, and A. Kuhn, *Phys. Rev. Lett.* **98**, 063601 (2007).
- [32] L. P. Parazzoli, A. M. Hankin, and G. W. Biedermann, *Phys. Rev. Lett.* **109**, 230401 (2012).
- [33] R. Bücker, A. Perrin, S. Manz, T. Betz, C. Koller, T. Plisson, J. Rottmann, T. Schumm, and J. Schmiedmayer, *New J. Phys.* **11**, 103039 (2009).
- [34] P. Storey and C. Cohen-Tannoudji, *J. Phys. II (France)* **4**, 1999 (1994).
- [35] C. J. Bordé, *Gen. Relativ. Gravit.* **36**, 475 (2004).
- [36] P. Wolf, L. Blanchet, C. J. Bordé, S. Reynaud, C. Salomon, and C. Cohen-Tannoudji, *Classical Quantum Gravity* **28**, 145017 (2011).
- [37] See Supplemental Material at <http://link.aps.org/supplemental/10.1103/PhysRevLett.120.043602> for details on the vSTIRAP dynamics, and for a discussion of the peculiar effects associated to the center of mass of the two-entangled-species state.
- [38] M. S. Chapman, T. D. Hammond, A. Lenef, J. Schmiedmayer, R. A. Rubenstein, E. Smith, and D. E. Pritchard, *Phys. Rev. Lett.* **75**, 3783 (1995).
- [39] C. Bordé, *Phys. Lett. A* **140**, 10 (1989).
- [40] M. A. Horne, A. Shimony, and A. Zeilinger, *Phys. Rev. Lett.* **62**, 2209 (1989).
- [41] J. G. Rarity and P. R. Tapster, *Phys. Rev. Lett.* **64**, 2495 (1990).
- [42] N. Schlosser, G. Reymond, and P. Grangier, *Phys. Rev. Lett.* **89**, 023005 (2002).
- [43] P. Xu, J. Yang, M. Liu, X. He, Y. Zeng, K. Wang, J. Wang, D. J. Papoular, G. V. Shlyapnikov, and M. Zhan, *Nat. Commun.* **6**, 7803 (2015).
- [44] G. S. Vasilev, D. Ljunggren, and A. Kuhn, *New J. Phys.* **12**, 063024 (2010).
- [45] N. V. Vitanov, A. A. Rangelov, B. W. Shore, and K. Bergmann, *Rev. Mod. Phys.* **89**, 015006 (2017).
- [46] See, for example, the single photon counting modules from Excelitas, <http://www.excelitas.com/Pages/Product/Single-Photon-Counting-Modules-SPCM.aspx>.
- [47] M. Mücke, J. Bochmann, C. Hahn, A. Neuzner, C. Nölleke, A. Reiserer, G. Rempe, and S. Ritter, *Phys. Rev. A* **87**, 063805 (2013).
- [48] We note further that the paths of the two isotopes can be made near identical by operating on the D2 line for ^{87}Rb and, e.g., rendering the emitted photons indistinguishable by wavelength conversion.
- [49] Isotope-dependent phase shifts must be carefully controlled. For example, the difference in magnetic field response of the two isotopes corresponds to a systematic effect of the order of 500 mrad for a magnetic field gradient of 1 mG cm^{-1} and $T = 50 \text{ ms}$, which must be controlled at the 2% level to achieve an accuracy of 5×10^{-8} on the Eötvös parameter.

- [50] More precisely, our scheme could be used to constrain the nondiagonal elements of the dimensionless operator $\hat{\eta} = \hat{I}_{\text{int}} - \hat{M}_g \hat{M}_i^{-1}$ defined in Ref. [24], and constrained at the level of 5×10^{-8} for a $\sim 30 \mu\text{eV}$ energy difference in Ref. [16].
- [51] M. Aspelmeyer, C. Brukner, D. Giulini, and G. Milburn, *New J. Phys.* **19**, 050401 (2017).
- [52] P. Dussarrat, M. Perrier, A. Imanaliev, R. Lopes, A. Aspect, M. Cheneau, D. Boiron, and C.I. Westbrook, *Phys. Rev. Lett.* **119**, 173202 (2017).